Binding the Mammalian High Mobility Group Protein AT-hook 2 to AT-Rich Deoxyoligonucleotides: Enthalpy-Entropy Compensation

Suzanne Joynt, Victor Morillo, and Fenfei Leng*
Department of Chemistry & Biochemistry, Florida International University, Miami, Florida 33199

ABSTRACT HMGA2 is a DNA minor-groove binding protein. We previously demonstrated that HMGA2 binds to AT-rich DNA with very high binding affinity where the binding of HMGA2 to poly(dA-dT)$_2$ is enthalpy-driven and to poly(dA)poly(dT) is entropy-driven. This is a typical example of enthalpy-entropy compensation. To further study enthalpy-entropy compensation of HMGA2, we used isothermal-titration-calorimetry to examine the interactions of HMGA2 with two AT-rich DNA hairpins: 5′-CCAAAAAAAA AAAAAAAGCCCCCGCTTTTTTTTTTTTTTTTGG-3′ (FL-AT-1) and 5′-CCATATATATATATATAGCCCCCGCTATATATATATAT ATGG-3′ (FL-AT-2). Surprisingly, we observed an atypical isothermal-titration-calorimetry-binding curve at low-salt aqueous solutions whereby the apparent binding-enthalpy decreased dramatically as the titration approached the end. This unusual behavior can be attributed to the DNA-annealing coupled to the ligand DNA-binding and is eliminated by increasing the salt concentration to ~200 mM. At this condition, HMGA2 binding to FL-AT-1 is entropy-driven and to FL-AT-2 is enthalpy-driven. Interestingly, the DNA-binding free energies for HMGA2 binding to both hairpins are almost temperature independent; however, the enthalpy-entropy changes are dependent on temperature, which is another aspect of enthalpy-entropy compensation. The heat capacity change for HMGA2 binding to FL-AT-1 and FL-AT-2 are almost identical, indicating that the solvent displacement and charge-charge interaction in the coupled folding/binding processes for both binding reactions are similar.

INTRODUCTION

The HMGA2 is a nuclear protein associated with mensenchymal cell development and differentiation (1–3). HMGA2 is only expressed in proliferating, undifferentiated mesenchymal cells and is undetectable in normal fully differentiated adult cells (1,4). Disruption of its normal expression patterns causes deregulations of cell growth and differentiation. For instance, *Hmga2* knock-out mice developed the pygmy phenotype (1). These mutant mice were severely deficient in fat cells and other mesenchymal tissues (almost a 20-fold decrease). Furthermore, it was demonstrated that disruption of the *Hmga2* gene caused a dramatic reduction in obesity of leptin-deficient mice (Lep^{ob}/Lep^{ob}) in a gene-dosage dependent manner: $Hmga2^{+/+}$ Lep^{ob}/Lep^{ob} mice weighed over three times more than $Hmga2^{-/-}$ Lep^{ob}/Lep^{ob} animals, and the weight of $Hmga2^{+/-}$ Lep^{ob}/Lep^{ob} mice was in between (2). These results suggest that HMGA2 plays an important role in fat-cell proliferation and is a potential target for the treatment of obesity (2). HMGA2 is also directly linked to the formation of various tumors, including malignant tumors such as lung cancer (5), hepatocellular carcinoma (6), prostate cancer (7), and leukemia (8); and benign tumors such as lipomas (9,10), uterine leiomyomas (11,12), and pulmonary chondroid hamartomas (13). Whereas rearrangements of chromosomal bands 12q13–15 where the HMGA2 gene is located are the main cause for the tumorigenesis of the benign tumors with mesenchymal origin (14,15), the over- and/or aberrant-expression of HMGA2 has been attributed to the formation of the malignant tumors (16–18). Intriguingly, the expression level of HMGA proteins, including HMGA2, often correlates with the degree of malignancy, the existence of metastasis, and a poor prognosis (19,20). These results suggest that HMGA proteins should be considered as diagnostic markers of metastatic potential and poor prognosis for many human carcinomas (14,16,17). These results also suggest that HMGA proteins are potential targets of microRNAs' therapy (21,22) and chemotherapy (17,23) for cancer patients.

HMGA2 is a DNA minor-groove binding protein and belongs to the HMGA protein family (24). Each protein in this family contains three small ''AT-hook'' DNA-binding motifs, which have a consensus core sequence, PRGRP, surrounded on each side with one or two positively charged amino acids, such as arginine or lysine. One unique feature of the AT-hook DNA-binding motifs is that, in the absence of DNA, they are natively ''disordered'' (25,26). However, when they bind to the minor-groove of the AT-rich DNA sequences, the AT-hooks adopt a well-defined structure. The RGR core penetrates into the minor-groove of AT-rich sequences with two arginine residues forming extensive contact with the floor of the minor-groove (26). The two prolines, on the other hand, direct the backbone of the peptide away from the minor-groove floor and position the positively charged arginine or lysine near the phosphates of DNA to make further contact. This ''disordered-to-ordered'' structural change upon binding to AT-rich DNA is very important for the AT-hook proteins, which allows

Submitted December 11, 2008, and accepted for publication February 9, 2009.

*Correspondence: lengf@fiu.edu

Abbreviations: DSC, differential scanning calorimetry; EMSA, electrophoretic mobility shift assay; HMGA2, the mammalian high mobility group protein AT-hook 2; ITC, isothermal titration calorimetry.

Editor: Jonathan B. Chaires.

0006-3495/09/05/4144/9 $2.00

doi: 10.1016/j.bpj.2009.02.015

them to participate in many essential nuclear activities, such as transcription (27,28), DNA replication (29), and DNA repair (30).

To understand how HMGA2 interacts with AT-rich DNAs, we have previously carried out various biochemical and biophysical studies (31,32). Our results demonstrated that HMGA2 is a sequence-specific DNA-binding protein and binds to AT-rich DNAs as a monomer (31). We also showed that HMGA2 binds to poly(dA-dT)$_2$ and poly(dA)poly(dT) with very high affinity in which the binding of HMGA2 to poly(dA-dT)$_2$ is enthalpy-driven and to poly(dA)poly(dT) is entropy-driven (32). This is a typical example of enthalpy-entropy compensation for a ligand binding to two different DNA substrates with similar binding free energies. In this study, we further examined enthalpy-entropy compensation using two AT-rich deoxyoligonucleotide hairpins: 5′-CCAAAAAAAAAAAAAAGCCCCCGCTTTTTTTTTTTTTTTTGG-3′ (FL-AT-1) and 5′-CCATATATATATATATAGCCCCCGCTATATATATATATATGG-3′ (FL-AT-2). Both oligomers contain a 15 bp AT sequence: FL-AT-1 contains a 15 bp A-tract; FL-AT-2 contains a 15 bp AT alternate sequence. To our surprise, our results showed unusual ITC curves in low-salt aqueous solutions, e.g., 1 × BPE containing 50 mM of NaCl. The apparent binding enthalpy decreased dramatically as the DNA approached depletion. Interestingly, our results showed that this unusual behavior was eliminated by increasing the salt concentration to ~200 mM NaCl. At this condition, e.g., 1 × BPE, 200 mM NaCl, HMGA2 binding to FL-AT-1 is entropy-driven and to FL-AT-2 is enthalpy-driven.

MATERIALS AND METHODS

Protein and DNA samples

HMGA2 was expressed and purified as described previously (32,33). An extinction coefficient of 5810 cm^{-1} M^{-1} was used to determine the HMGA2 concentration. Synthetic deoxyoligonucleotides, FL-AT-1, FL-AT-2, FL238, and FL239 were purchased from MWG-Biotech, Inc. (High Point, NC). DNA oligonucleotides were annealed in a 4 L water bath, which was heated to 98°C for 10 min and slowly cooled to room temperature.

ITC

ITC experiments were carried out using a VP-ITC titration calorimeter (MicroCal LLC, Northampton, MA). Samples were extensively dialyzed against 1 × BPE buffer containing 200 mM NaCl or the indicated salt concentration. Typically, the titration was set up so that 15 μL of 35.7 μM HMGA2 was injected every 200 seconds, up to a total of 18 injections, into a DNA sample (1.44 mL of 100 μM (bp)) in the sample cell. The heat liberated or absorbed with each injection of ligand is observed as a peak that corresponds to the power required to keep the sample and reference cells at identical temperatures. The peaks produced over the course of a titration are converted to heat output per injection by integration and corrected for cell volume and sample concentration. Control experiments were carried out to determine the contribution to the measurement by the heats of dilution arising from (1) protein into buffer and (2) buffer into DNA. The net enthalpy for each protein-DNA interaction was determined by subtraction of the component heats of dilution. The ITC data was fitted using the built-in curve fitting model for a single set of identical binding sites to obtain the DNA-binding constant and other thermodynamic parameters.

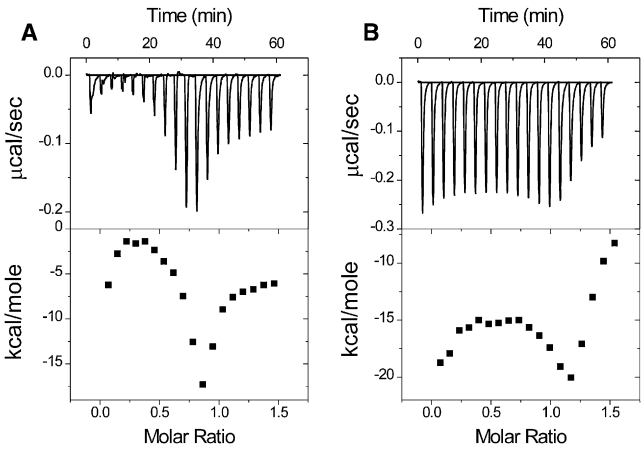

FIGURE 1 The unusual ITC-binding curves under a low-salt condition. Sample raw data for the titration of HMGA2 into FL-AT-1 (*A*) and FL-AT-2 (*B*) at 25°C in 1 × BPE containing 50 mM of NaCl (total 66 mM Na^+). Top: each peak shows the heat produced by injection of an aliquot of 15 μL of HMGA2 (35.7 μM) into DNA solution (1.44 mL of 5 μM). Bottom: the binding isotherm generated from integration with respect of time with appropriate dilution correction.

DSC

DSC experiments were carried out using a VP-DSC calorimeter (MicroCal LLC). Samples were extensively dialyzed against 1 × BPE buffer containing 50 mM or 200 mM of NaCl. DSC scans were conducted between 0°C and 110°C at a rate of 60°C per hour. Baselines, obtained by filling both calorimeter cells with the corresponding buffer, were subtracted from the sample experimental thermograms.

EMSA

EMSA experiments were performed as previously described (31). The AT-rich DNA oligomer FL-AT-3 was annealed from two complementary single-stranded deoxyoligonucleotides, FL238 (5′-AAAAATTTTTAAAAA-3′) and FL239 (5′-TTTTTAAAAATTTTT-3′) in 20 mM Tris-HCl (pH 8.0), 50 mM NaCl, and 1 mM EDTA. The protein-DNA complexes were formed by addition of appropriate amounts of the protein to a solution containing 200 nM of FL-AT-3 in the 1 × DNA-binding buffer containing 20 mM Tris-HCl (pH 8.0), 50 mM NaCl, 0.5 mM EDTA, 1 mM dithiothreitol, 0.5 mM $MgCl_2$, and 5% glycerol. After equilibration for 60 min at 24°C, the samples were loaded on a 12% native polyacryamide gel in 0.5 × TBE buffer (0.045 M Tris-Borate, pH 8.3 and 1 mM EDTA) to separate free and bound DNA.

RESULTS

The unusual ITC titration curves of HMGA2 binding to AT-rich DNA oligonucleotides under low-salt buffer conditions

ITC was used to investigate the DNA-binding properties of HMGA2 binding to the AT-rich DNA hairpins FL-AT-1 and FL-AT-2. Fig. 1 shows the results of HMGA2 titrating into FL-AT-1 and FL-AT-2 solutions in 1 × BPE containing

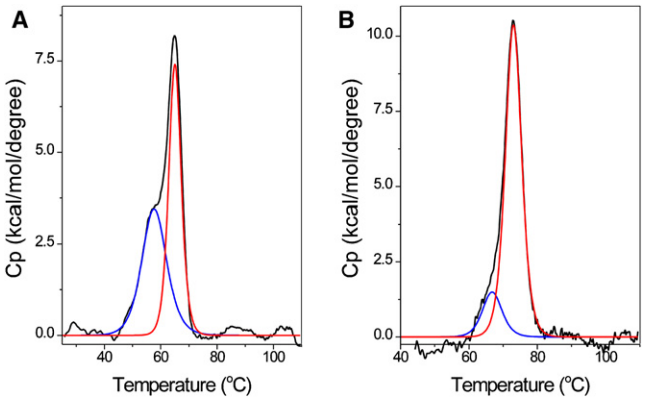

FIGURE 2 The DSC thermograms of the AT-rich DNA FL-AT-1 in 1 × BPE containing 50 mM (*A*) or 200 mM (*B*) of NaCl. The molar heat capacity (C_p) is plotted against temperature after baseline correction. The deconvolution of the two overlapping peaks is also shown (*red and blue lines*).

50 mM NaCl (total 66 mM of Na^+). Both titration curves are quite unusual. The enthalpy initially increased, then decreased, and finally increased again. These results suggest that more than one reaction exists in the ITC experiments. The existence of multiple nonidentical binding sites could explain the observed behavior, but it is known that there is only a single binding site of HMGA2 in these two oligomers (31,32). In this case, it is unlikely that the unusual ITC titration curves are results of HMGA2 binding to different HMGA2 sites on these two oligomers. Another possibility is that the unusual binding curves may result from the coupled-annealing of the oligomers to HMGA2 binding. Because FL-AT-1 and FL-AT-2 are AT-rich oligonucleotides, a small amount of the oligomers may be partially annealed at relatively low-salt concentrations (see later discussion for details). The binding of HMGA2 to both oligomers should shift the equilibrium toward the annealed status, especially near the end of the binding reaction. As demonstrated previously, the annealing of oligonucleotides is an exothermal reaction (34,35). Therefore, as the binding reaction nears the end, a decrease of the binding enthalpy may be observed. If this possibility is the case, the unusual ITC binding curves should depend on the salt concentration and the reaction temperature, i.e., a relatively high-salt concentration and/or a relatively low temperature should give normal ITC binding curves for HMGA2 binding to these two AT-rich oligomers (a ''normal'' ITC curve refers to a thermogram resulting from a binding reaction with a single set of identical binding sites). Indeed, our results shown in Figs. S1 and S2 in the Supporting Material demonstrated that the atypical ITC curves can be converted to the normal ITC curves at a high-salt concentration or a low temperature (compare Fig. S1, *A* and *B*; also compare Fig. S2, *A* and *B*). For example, in 1 × BPE buffer containing 150 mM of NaCl at 5°C and 15°C, titrating HMGA2 into FL-AT-1 results in normal ITC curves with a stoichiometry of 1:1 and the DNA-binding constant of 1.0 and 1.4 × 10^8 M^{-1}, respectively. Similar results were also obtained for oligomer FL-AT-2 (data not shown).

TABLE 1 DNA melting temperatures and melting enthalpies of FL-AT-1 in 1 × BPE containing 50 or 200 mM of NaCl

[NaCl]	T_m	(°C)	ΔH	(kcal mol^{-1})
mM	T_1	T_2	ΔH_1	ΔH_2
50	58.0	65.1	62.1	80.5
200	66.4	73.0	39.1	124.2

The DNA melting temperatures and melting enthalpies of FL-AT-1 were determined from DSC experiments as shown in Fig. 4.

We also performed DSC experiments to study the thermal stability of oligomer FL-AT-1 in two different salt concentrations: 50 and 200 mM of NaCl. Fig. 2 shows our DSC results. After baseline subtraction, the DSC thermograms were deconvoluted into two overlapping transitions for FL-AT-1 in both salt concentrations. These results suggest that two conformers, a partially annealed and a fully annealed conformer of FL-AT-1 exist in the solutions. The first and second transitions of the DSC thermograms should come from these two FL-AT-1 conformers, respectively. As expected, the T_m values of FL-AT-1 in 200 mM of NaCl are higher than those in 50 mM of NaCl (66.4 ± 1.9 and 73.0 ± 0.2°C for 200 mM of NaCl; 58.0 ± 0.4 and 65.1 ± 0.1°C for 50 mM of NaCl; Table 1). Intriguingly, although the total melting enthalpy values of FL-AT-1 under the two salt conditions are similar, the melting enthalpies of FL-AT-1 for each transition are different (Table 1). The melting enthalpies of FL-AT-1 were determined to be 62.1 and 80.5 kcal mol^{-1} for the first and second transitions, respectively, in 1 × BPE containing 50 mM of NaCl. In contrast, the melting enthalpies of FL-AT-1 are 39.1 and 124.2 kcal mol^{-1} for the first and second transitions, respectively, in 1 × BPE containing 200 mM of NaCl. If we assume that the enthalpy value is proportional to the amount of the conformers in the solutions, these results suggest that the partially annealed conformer of FL-AT-1 can be converted into the fully annealed conformer upon increasing the salt concentration. In other words, in 1 × BPE containing 50 mM of NaCl, almost half of FL-AT-1 is in a partially annealed status in the temperature near T_m (we believe that the amount of FL-AT-1 in the partially annealed status is much less at 25°C). In contrast, in 1 × BPE containing 200 mM of NaCl, most of FL-AT-1 (~80%) is fully annealed around T_m. These results suggest that the unusual ITC curves may come from the partially annealed DNA conformer, and the ITC titration experiments should be performed in 1 × BPE containing 200 mM of NaCl. Similar results were also obtained by using FL-AT-2 as the DNA oligomer (data not shown).

So far, we only used the DNA hairpins for our ITC experiments. As demonstrated previously, DNA hairpins are thermally more stable than the DNA duplexes derived from the complementary strands (36–38). Therefore, we decided to perform some ITC experiments by using an

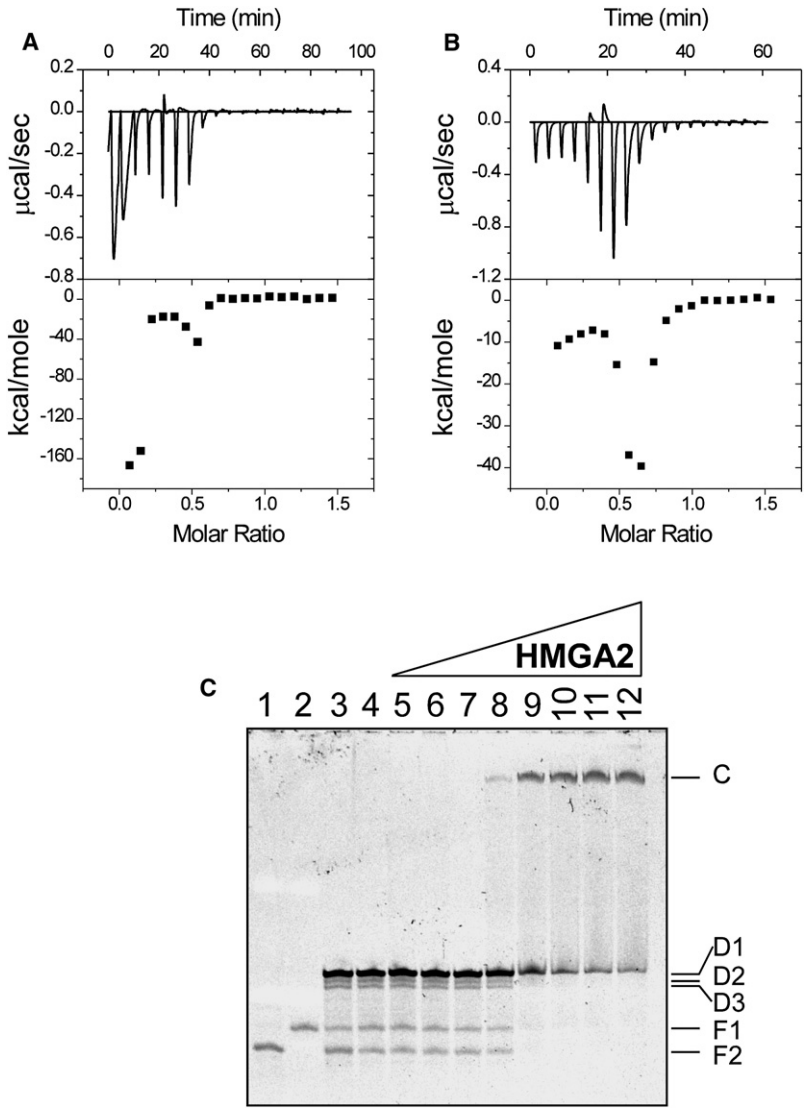

FIGURE 3 The annealing of the AT-rich oligomer FL-AT-3 is coupled to the binding of HMGA2 to DNA. Sample raw data for the titration of HMGA2 into FL-AT-3 at 25°C in 1 × BPE containing (*A*) 50 mM or (*B*) 100 mM of NaCl. Top: each peak shows the heat produced by injection of an aliquot of 15 μL of HMGA2 (35.7 μM) into DNA solution (1.44 mL of 5 μM). Bottom: the binding isotherm generated from integration with respect of time with appropriate dilution correction. (*C*) EMSA experiments for binding HMGA2 to FL-AT-3. The preannealed FL-AT-3 (200 nM) was incubated with increasing concentrations of HMGA2 in 50 μL of 1 × DNA binding buffer containing 20 mM Tris-HCl (pH 8.0), 50 mM NaCl, 0.5 mM EDTA, 1 mM dithiothretiol, and 5% glycerol. EMSA experiments were performed as described under Materials and Methods. After staining with nucleic acid stain SYBR Gold, the gels were visualized and photographed under ultraviolet light. Lanes 1 and 2 represent the single-stranded oligomer FL-238 and FL-239, respectively. Lanes 3 and 4 are the free FL-AT-3. In addition to FL-AT-3, lanes 5–12 also contain 50, 100, 200, 500, 1000, 2000, 5000, and 10,000 nM of HMGA2, respectively. Labels: F1, the free single stranded FL239; F2, the free single-stranded FL238; D1, the fully annealed FL-AT-3; D2 and D3, the partially annealed FL-AT-3; C, the HMGA2-FL-AT-3 complex.

AT-rich dsDNA oligomer as the DNA template. A 15 bp AT-rich oligomer (FL-AT-3) was used (the top strand: 5′-AAAAATTTTTAAAAA-3′). Fig. 3, *A* and *B* shows the results of the ITC experiments in 1 × BPE containing 50 and 100 mM of NaCl, respectively. Surprisingly, a very large negative binding enthalpy (~−160 kcal mol^{-1}) was obtained for the first two injections of the ITC experiment in 1 × BPE containing 50 mM of NaCl (Fig. 3 *A*). The enthalpy then increased to ~ −20 kcal mol^{-1}, decreased, and increased again. When the NaCl concentration was increased to 100 mM, we did not get the large negative enthalpies for the first two injections (Fig. 3 *B*). Nevertheless, the ITC titration curve is similar to the ITC curves shown in Fig. 1. (Similar results were obtained by decreasing temperature to 15°C as well (data not shown)). We also used EMSA to study HMGA2 binding to FL-AT-3. In this experiment, HMGA2 was titrated into a solution containing 200 nM of FL-AT-3 in 20 mM Tris-HCl (pH 8.0) and 50 mM of NaCl. In the absence of HMGA2, FL-AT-3 was partially dissociated into single-stranded DNA (compare lanes 1 and 2 to lanes 3 and 4 of Fig. 3 *C*). Furthermore, three additional bands, which represent the double-stranded FL-AT-3, appeared in the gel. This result suggests that FL-AT-3 exists in solution in at least three different states: single-stranded, partially annealed, and fully annealed states. When HMGA2 bound to FL-AT-3, the single-stranded DNA and two minor species of the partially annealed dsDNA disappeared (compare lanes 3 to 6 with lanes 8 to 12 of Fig. 3 *C*); simultaneously, one shift band corresponding to the HMGA2-DNA complex appeared. These results strongly suggest that the binding of HMGA2 to FL-AT-3 drove the equilibrium toward the formation of the fully-annealed dsDNA.

The binding of HMGA2 to FL-AT-1 is an entropy-driven reaction

At this stage, our results showed that the optimal condition for our ITC experiments is in 1 × BPE containing 200 mM of

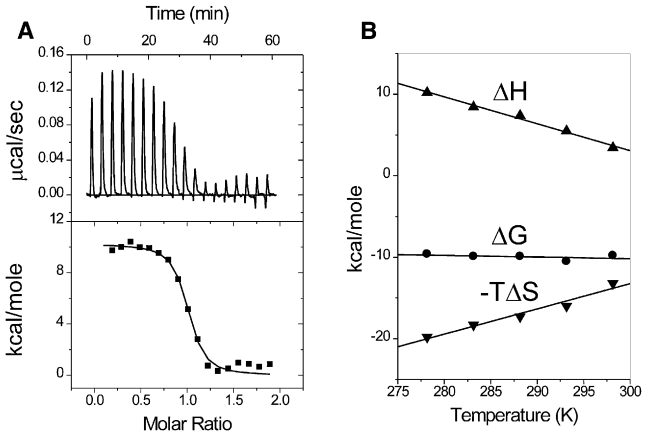

FIGURE 4 The binding of HMGA2 to FL-AT-1 is an entropy-driven reaction. (*A*) Sample raw data for the titration of HMGA2 into FL-AT-1 at 5°C in 1 × BPE containing 200 mM of NaCl (total 216 mM Na^+). Top: each peak shows the heat produced by injection of an aliquot of 15 μL of HMGA2 (35.7 μM) into DNA solution (1.44 mL of 5 μM). Bottom: the binding isotherm generated from integration with respect of time with appropriate dilution correction. (*B*) Heat capacity change (ΔC_p) for binding HMGA2 to FL-AT-1. Linear least-squares fitting of the enthalpy data (*up triangles*) determined by ITC giving a ΔC_p value of −330 (±30) cal mol^{-1} K^{-1}. The dependence of ΔG (*circles*) and $-T\Delta S$ (*down triangles*) on temperature are shown. The standard deviation of ΔH at different temperatures was estimated to be 0.1 (5°C), 0.1 (10°C), 0.2 (15°C), 0.3 (20°C), and 0.2 (25°C) kcal mol^{-1}, respectively.

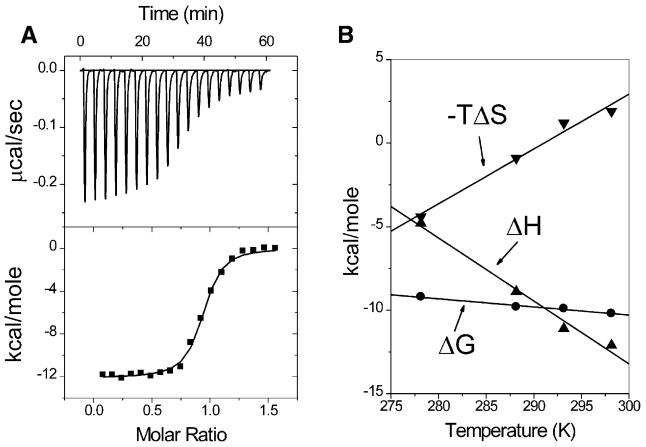

FIGURE 5 The binding of HMGA2 to FL-AT-2 is an enthalpy-driven reaction. (*A*) Sample raw data for the titration of HMGA2 into FL-AT-2 at 25°C in 1 × BPE containing 200 mM of NaCl (total 216 mM Na^+). Top: each peak shows the heat produced by injection of an aliquot of 15 μL of HMGA2 (35.7 μM) into DNA solution (1.44 mL of 5 μM). Bottom: the binding isotherm generated from integration with respect of time with appropriate dilution correction. (*B*) Heat capacity change (ΔC_p) for binding HMGA2 to FL-AT-2. Linear least-squares fitting of the enthalpy data (*up triangles*) determined by ITC giving a ΔC_p value of −377 (±50) cal mol^{-1} K^{-1}. The dependence of ΔG (*circles*) and $-T\Delta S$ (*down triangles*) on temperature are shown. The standard deviation of ΔH at different temperatures was estimated to be 0.2 (5°C), 0.3 (10°C), 0.2 (15°C), 0.3 (20°C), and 0.1 (25°C) kcal mol^{-1}, respectively.

NaCl. Under this condition, the DNA-binding enthalpy, the DNA-binding stoichiometry, and the DNA-binding constant can be measured directly. Fig. 4 *A* shows results from the ITC experiment in which HMGA2 was titrated into FL-AT-1 in 1 × BPE containing 200 mM NaCl at 5°C. Binding of HMGA2 to FL-AT-1 is an endothermic reaction, which yields a positive enthalpy of +10.2 (±0.2) kcal mol^{-1}. The binding constant and the binding stoichiometry were determined to be 3.4 (±0.9) × 10^7 M^{-1} and 1:1, respectively. The DNA-binding free energy and entropy were calculated to be −9.6 (±2.5) kcal mol^{-1} and +71.2 cal mol^{-1} K^{-1}, respectively. These results clearly showed that the binding of HMGA2 to FL-AT-1 is an entropy-driven reaction.

ΔH values for the interaction of HMGA2 with FL-AT-1 were determined at different temperatures (from 5°C to 25°C) by ITC. Fig. 4 *B* shows the results in which the slope of a linear least-squares fit gives a value of ΔC_p, $d\Delta H/dT$ of −330 (±30) cal mol^{-1} K^{-1}. The free energy of DNA-binding was calculated from $\Delta G = -RTlnK$ in which the DNA-binding constant was also determined from the ITC experiments. Interestingly, the free energy change is less sensitive to temperature than the DNA-binding enthalpy ΔH. The DNA-binding enthalpy is linearly compensated by the DNA-binding entropy, which results in relatively small changes of the free energy. Our results are summarized in Table 2.

TABLE 2 Comparison of thermodynamic parameters for HMGA2 binding to FL-AT-1 and FL-AT-2

DNA	K_{obs}	ΔG_{obs}	ΔH	$-T\Delta S$	ΔC_p
FL-AT-1	1.6×10^7	−9.8	3.4	−13.4	−330
FL-AT-2	2.9×10^7	−10.2	−12.1	1.9	−377

K_{obs} (M^{-1}) is the binding constant for the interaction of HMGA2 with DNA and refers to solutions containing 0.20 M NaCl at 25°C. ΔG_{obs} (kcal mol^{-1}) is the binding free energy calculated from the equation $\Delta G_{obs} = -RTlnK_{obs}$. The DNA-binding enthalpy ΔH was determined by ITC experiments. $-T\Delta S$ was calculated by subtraction, $-T\Delta S = \Delta G - \Delta H$.

The binding of HMGA2 to FL-AT-2 is an enthalpy-driven reaction

Fig. 5 *A* shows results from the ITC experiment in which HMGA2 was titrated into a solution containing FL-AT-2 and 200 mM NaCl at 25°C. The binding of HMGA2 to FL-AT-2 is an exothermic reaction, producing a negative enthalpy of −12.1 (±0.1) kcal mol^{-1}. The binding constant and the binding stoichiometry were determined to be 2.9 (±0.4) × 10^7 M^{-1} and 1:1, respectively. The DNA-binding free energy and entropy were calculated to be −10.2 (±1.4) kcal mol^{-1} and +6.6 cal $mol^{-1}K^{-1}$, respectively. In contrast to HMGA2 binding to FL-AT-1, the binding of HMGA2 to FL-AT-2 is an enthalpy-driven reaction.

ΔH values for the interaction between HMGA2 and FL-AT-2 were also determined at different temperatures by ITC experiments (Fig. 5 *B*). The slope of a linear least-squares fit yields a value of ΔC_p of −377 (±50) cal mol^{-1} K^{-1}. As expected, the calculated DNA-binding free energy change is less sensitive to temperature than ΔH. The values

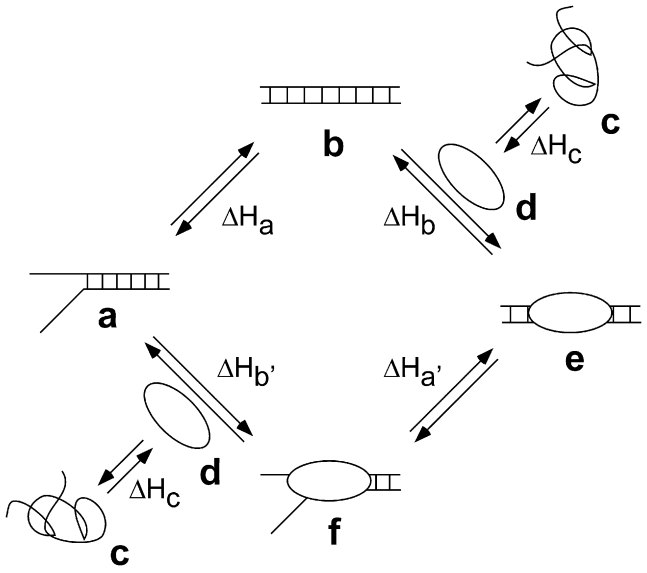

FIGURE 6 A coupled DNA-annealing model to explain the unusual ITC titration curves for HMGA2 binding to AT-rich DNA oligomers. *a* to *f* represent the partially annealed DNA oligomer, the fully annealed DNA oligomer, the partially unfolded protein, the fully folded protein, the protein-DNA complex with the fully annealed oligomer, the protein-DNA complex with the partially annealed oligomer, respectively. ΔH_a, ΔH_b, ΔH_c, ΔH_a', and ΔH_b' represents the enthalpy change associated with each step.

of ΔH and ΔS are linearly correlated, and the change in enthalpy is compensated by changes in the entropy to yield small changes of the free energy. These results also summarized in Table 2.

DISCUSSION

In this study, we demonstrated that the ITC curves of HMGA2 binding to all three AT-rich oligomers, FL-AT-1, FL-AT-2, and FL-AT-3 are quite unusual at low-salt concentrations. The binding enthalpy initially increased, then decreased, and finally increased again (Fig. 1 and Figs. S1, S2, and S3). We also showed that these unusual ITC curves are dependent on the salt concentration and temperature (Figs. S1 and S2). We believe that this unusual ITC behavior can be best explained by a coupled DNA-annealing model shown in Fig. 6. The AT-rich DNA oligomers, under low-salt buffer conditions, should be a mixture of partially and fully annealed oligomers (Fig. 6, *a* and *b*). If HMGA2 only binds to the fully annealed oligomers (Fig. 6 *b*), the binding of HMGA2 to the AT-rich oligomers should shift the equilibrium to the side of the fully annealed DNA. In this case, $\Delta H_{obs} = \Delta H_a + \Delta H_b + \Delta H_c$, whereby ΔH_{obs}, ΔH_a, ΔH_b, and ΔH_c are the observed enthalpy change, the annealing enthalpy of the partially annealed DNA oligomer, the DNA-binding enthalpy of HMGA2, and the protein-folding enthalpy of HMGA2, respectively. Because HMGA2 is a natively unfolded protein (25,26), the protein folding enthalpy ΔH_c should be equal to 0, i.e., $\Delta H_c = 0$ (ΔH_c does not include the enthalpy change associated with the protein conformation change upon binding to DNA, which cannot be differentiated from the DNA-binding enthalpy, i.e., ΔH_b); therefore, $\Delta H_{obs} = \Delta H_a + \Delta H_b$. In any case, ΔH_a should be proportional to the amount of partially annealed DNA oligomers in solution and thus sensitive to the experimental conditions, such as salt concentration and temperature. Indeed, our DSC results showed that the amount of partially annealed DNA oligomer is a function of the salt concentration (Fig. 2). Therefore, ΔH_a can be minimized by increasing the salt concentration or by decreasing the experimental temperature. As demonstrated previously, DNA annealing is an exothermic reaction (34,35), i.e., $\Delta H_a < 0$. If the amount of the partially annealed DNA oligomer is significant in the ITC experiment, ΔH_{obs} will be much lower than ΔH_b, especially near the end of the reaction. This is probably the reason why a decrease of the binding enthalpy is always observed as the binding reaction approaches the end under the low-salt buffer conditions. An alternative pathway of the coupled DNA-annealing model is also shown in Fig. 6. As the titration approaches the end, the fully annealed DNA oligomer is depleted. In this case, HMGA2 binds to the partially annealed DNA oligomer to drive the partially annealed form (Fig. 6 *f*) into the fully annealed form (Fig. 6 *e*). If $\Delta H_b' + \Delta H_a' < \Delta H_b$, a decrease of the apparent binding enthalpy should be observed in the end of the titration.

The most direct evidence to support the coupled DNA-annealing model comes from the results of the ITC and EMSA experiments using the AT-rich oligomer FL-AT-3 (Fig. 3). In the solution containing 50 mM of NaCl, FL-AT-3 exists in three different forms: the single-stranded, the partially annealed, and the fully annealed form (Fig. 3 *C*). The single-stranded and partially annealed FL-AT-3 can be converted to the fully annealed form of FL-AT-3 upon binding to HMGA2 (Fig. 3 *C*). Intriguingly, the enthalpy change of the first two injections of the ITC experiment at 50 mM of NaCl is so large and cannot be explained from the contribution of the binding of HMGA2 to FL-AT-3. Instead, the large enthalpy change may stem from the annealing of the two complementary single-stranded strands of FL-AT-3 into the double-stranded DNA, which is coupled to the binding of HMGA2 to FL-AT-3, because, under this condition, a significant amount of FL-AT-3 is single stranded (Fig. 3 *C*). Increasing the salt concentration to 100 mM resulted in a much smaller enthalpy change for the first two injections of the ITC experiment (compare Fig. 3, *A* to *B*). These results suggest that the unusual ITC curves are the result of the coupling reaction between the binding of HMGA2 to DNA and the annealing of the unpaired DNA strands.

Similar unusual results were observed by Fodor and Ginsburg (39) during the ITC titration of the cardiac-specific homeodomain NK × 2.5(C56S) protein into a solution containing a specific 18 bp DNA oligomer. They also found

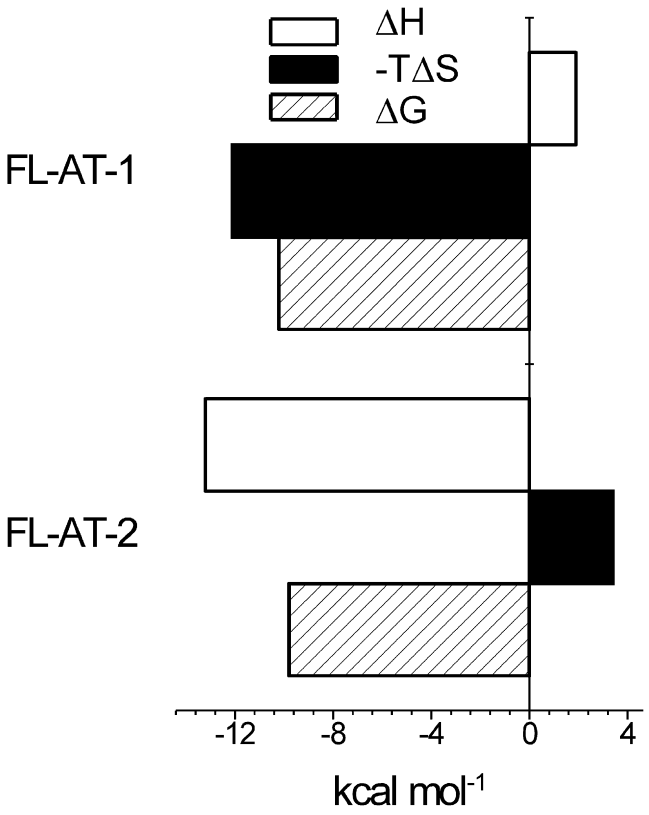

FIGURE 7 Comparison of the thermodynamic profiles for HMGA2 binding to FL-AT-1 and FL-AT-2.

a large sudden decrease in enthalpy as the free DNA neared depletion, when the temperature of the ITC experiment was sufficiently high. The sudden decrease of the binding enthalpy was attributed to the refolding of the impaired DNA or unfolded protein, which is consistent with our interpretation. The only difference is that HMGA2 is a natively unfolded protein, and the oligomers used in our ITC experiments are AT-rich. In our case, the decrease of the binding enthalpy should come exclusively from the annealing of the unannealed DNA basepairs, and protein folding should not be a factor. There are a few cases of unusual ITC curves for the binding of small ligands to DNA (40–42). For example, the titration of the minor-groove binder, netropsin, into a few DNA hairpins yielded rather complex ITC curves (40) that were fit and explained by a ''two-fractional-sites'' model. In this model, the total number of sites is one netropsin per DNA molecule, but the two fractional sites have relative stoichiometries. We have noticed some differences between our ITC data and the results of netropsin titrating into DNA hairpins. For instance, the magnitude of the enthalpy decrease in our ITC experiments is much larger as the free DNA approaches depletion. In addition, HMGA2 is a macromolecule, and the DNA hairpins used in this study are AT-rich. Nevertheless, we cannot rule out the possibility that the unusual ITC behaviors in our ITC experiments are the results of the existence of two fractional sites for HMGA2.

In this study, we clearly demonstrated that HMGA2 uses different driving forces to interact with different DNA substrates (Fig. 7). At 25°C in 1 × BPE containing 200 mM of NaCl, HMGA2 binding to FL-AT-1 is exclusively entropy-driven with an unfavorable ΔH of +3.4 kcal mol^{-1}, a ΔG of −9.8 kcal mol^{-1}, and a favorable ΔS of +44.5 cal mol^{-1} K^{-1} ($-T\Delta S$, −13.2 kcal mol^{-1}). In contrast, under the same experimental condition, HMGA2 binding to FL-AT-2 is overwhelmingly enthalpy driven with a favorable ΔH of −12.1 kcal mol^{-1}, a ΔG of −10.2 kcal mol^{-1}, and a small unfavorable ΔS of −6.6 cal mol^{-1} K^{-1} ($-T\Delta S$, +1.9 kcal mol^{-1}). Similar to HMGA2 binding to poly(dA)poly(dT) and poly(dA-dT)$_2$ (32), this is another example of isothermal enthalpy-entropy compensation for one ligand binding to two different substrates (43). A possible reason for the enthalpy-entropy compensation is that the HMGA2-FL-AT-1 complex is more dehydrated than the HMGA2-FL-AT-2 complex, i.e., HMGA2 binding to FL-AT-1 releases more water molecules than its binding to FL-AT-2 (44). Alternatively, the binding of HMGA2 to FL-AT-1, an A-tract molecule, may result in a conformational transition in FL-AT-1, which is specific for the A-tracts (45). The positive binding enthalpy may come from the helix-to-helix transition of the A-tract. Regardless, the coupled DNA conformation transition is directly linked to the disruption of hydration in the minor-groove of FL-AT-1 (45). In this study, our data also showed that the binding free energies for HMGA2 binding to both AT-rich DNA hairpins are almost independent of temperature (~−10 kcal mol^{-1}). However, the enthalpy and entropy changes are highly dependent on the temperature, which is another aspect of enthalpy-entropy compensation. As pointed out by Sharp (46), this temperature-dependent enthalpy-entropy compensation is a restatement of the thermodynamic definition of $\Delta C_p = \frac{d\Delta H}{dT} = \frac{d\Delta S}{dT}$ at constant pressure. Because ΔC_p for HMGA2 binding to the two hairpins is temperature independent, a plot of ΔH versus ΔS at different temperatures appears linear. A likely molecular interpretation of the temperature-dependent enthalpy-entropy compensation in our system is that the more favorable binding-entropy at lower temperatures is mainly due to the ΔS component associated with the displacement of water molecules in the minor-groove. At lower temperatures, it takes more heat or greater enthalpy to ''melt'' the ordered, ice-like molecules in the minor-groove (47). As a result, it will generate more favorable entropic changes to drive the binding reaction to completion.

As demonstrated previously (32), HMGA2 binding to poly(dA-dT)$_2$ is accompanied by a large negative heat capacity change (ΔC_p, −705 ± 113 cal mol^{-1} K^{-1}) in 1 × BPE containing 4 mM of NaCl (total 20 mM Na^+). We attributed this large ΔC_p to three components: the dehydration of the groups in the interface between HMGA2 and DNA, the protein folding induced by DNA-binding, and the charge-charge (electrostatic) interaction in the minor-groove between the highly positively charged HMGA2 and

the highly negatively charged DNA (32). We believe that the contribution of the electrostatic interaction (Coulombic forces) to ΔC_p is substantial and should decrease strongly with increasing salt concentration. Indeed, our results showed that ΔC_p is ~−350 cal mol^{-1} K^{-1} for HMGA2 binding to both AT-rich hairpins, FL-AT-1 and FL-AT-2, in 1 × BPE containing 200 mM of NaCl (total 216 mM Na^+) and significantly smaller than ΔC_p determined in the solution containing 20 mM of Na^+ in our previous study (32). These results suggest that the charge-charge interaction plays a key role in HMGA2 binding to AT-rich DNAs. Interestingly, an almost identical ΔC_p value was obtained for HMGA2 binding to different oligomers, FL-AT-1 (−330 (±30) cal mol^{-1} K^{-1}) and FL-AT-2 (−377 (±50) cal mol^{-1} K^{-1}). These results suggest that the solvent displacement and charge-charge interaction in the coupled folding/binding processes for these binding reactions are similar.

SUPPORTING MATERIAL

Two figures are available at http://www.biophysj.org/biophysj/supplemental/S0006-3495(09)00568-2.

The authors thank Dr. Tengjiao Cui for performing EMSA experiments. We also thank Dr. Watson Lees (Florida International University) for his thoughtful comments to improve the quality of this article.

F.L. acknowledges National Institutes of Health grant S06 GM008205 (to F.L.) and Department of Defense grant 49498-CH-HIS (to Ramon Lopez and F.L.). V. Morillo was supported by the Minority Opportunities in Research Programs Research Initiative for Scientific Enhancement Program at Florida International University (National Institutes of Health Grant R25 GM).

REFERENCES

1. Zhou, X., K. F. Benson, H. R. Ashar, and K. Chada. 1995. Mutation responsible for the mouse pygmy phenotype in the developmentally regulated factor HMGI-C. *Nature*. 376:771–774.
2. Anand, A., and K. Chada. 2000. In vivo modulation of Hmgic reduces obesity. *Nat. Genet*. 24:377–380.
3. Reeves, R. 2003. HMGA proteins: flexibility finds a nuclear niche? *Biochem. Cell Biol*. 81:185–195.
4. Gattas, G. J., B. J. Quade, R. A. Nowak, and C. C. Morton. 1999. HMGIC expression in human adult and fetal tissues and in uterine leiomyomata. *Genes Chromosomes Cancer*. 25:316–322.
5. Sarhadi, V., H. Wikman, K. Salmenkivi, E. Kuosma, T. Sioris, J. Salo, A. Karjalainen, S. Knuutila, and S. Anttila. 2006. Increased expression of high mobility group A proteins in lung cancer. *J. Pathol* 209:206–212.
6. Chang, Z. G., L. Y. Yang, W. Wang, J. X. Peng, G. W. Huang, et al. 2005. Determination of high mobility group A1 (HMGA1) expression in hepatocellular carcinoma: a potential prognostic marker. *Dig. Dis. Sci*. 50:1764–1770.
7. Tamimi, Y., H. G. van der Poel, H. F. Karthaus, F. M. Debruyne, and J. A. Schalken. 1996. A retrospective study of high mobility group protein I(Y) as progression marker for prostate cancer determined by in situ hybridization. *Br. J. Cancer*. 74:573–578.
8. Kottickal, L. V., B. Sarada, H. Ashar, K. Chada, and L. Nagarajan. 1998. Preferential expression of HMGI-C isoforms lacking the acidic carboxy terminal in human leukemia. *Biochem. Biophys. Res. Commun*. 242:452–456.
9. Ashar, H. R., M. S. Fejzo, A. Tkachenko, X. Zhou, J. A. Fletcher, et al. 1995. Disruption of the architectural factor HMGI-C: DNA-binding AT hook motifs fused in lipomas to distinct transcriptional regulatory domains. *Cell*. 82:57–65.
10. Schoenmakers, E. F., S. Wanschura, R. Mols, J. Bullerdiek, B. H. Van den Berghe, and W. J. Van de Ven. 1995. Recurrent rearrangements in the high mobility group protein gene, HMGI- C, in benign mesenchymal tumours. *Nat. Genet*. 10:436–444.
11. Schoenmakers, E. F., C. Huysmans, and W. J. Van de Ven. 1999. Allelic knockout of novel splice variants of human recombination repair gene RAD51B in t(12;14) uterine leiomyomas. *Cancer Res*. 59:19–23.
12. Klotzbucher, M., A. Wasserfall, and U. Fuhrmann. 1999. Misexpression of wild-type and truncated isoforms of the high-mobility group I proteins HMGI-C and HMGI(Y) in uterine leiomyomas. *Am. J. Pathol*. 155:1535–1542.
13. Kazmierczak, B., J. Rosigkeit, S. Wanschura, K. Meyer-Bolte, W. J. Van de Ven, et al. 1996. HMGI-C rearrangements as the molecular basis for the majority of pulmonary chondroid hamartomas: a survey of 30 tumors. *Oncogene*. 12:515–521.
14. Tallini, G., and P. Dal Cin. 1999. HMGI(Y) and HMGI-C dysregulation: a common occurrence in human tumors. *Adv. Anat. Pathol*. 6:237–246.
15. Aman, P. 1999. Fusion genes in solid tumors. *Semin. Cancer Biol*. 9:303–318.
16. Young, A. R., and M. Narita. 2007. Oncogenic HMGA2: short or small? *Genes Dev*. 21:1005–1009.
17. Fusco, A., and M. Fedele. 2007. Roles of HMGA proteins in cancer. *Nat. Rev. Cancer*. 7:899–910.
18. Chiappetta, G., A. Ferraro, E. Vuttariello, M. Monaco, F. Galdiero, et al. 2008. HMGA2 mRNA expression correlates with the malignant phenotype in human thyroid neoplasias. *Eur. J. Cancer*. 44:1015–1021.
19. Abe, N., T. Watanabe, M. Sugiyama, H. Uchimura, G. Chiappetta, et al. 1999. Determination of high mobility group I(Y) expression level in colorectal neoplasias: a potential diagnostic marker. *Cancer Res*. 59:1169–1174.
20. Meyer, B., S. Loeschke, A. Schultze, T. Weigel, M. Sandkamp, et al. 2007. HMGA2 overexpression in non-small cell lung cancer. *Mol. Carcinog*. 46:503–511.
21. Kumar, M. S., S. J. Erkeland, R. E. Pester, C. Y. Chen, M. S. Ebert, et al. 2008. Suppression of non-small cell lung tumor development by the let-7 microRNA family. *Proc. Natl. Acad. Sci. USA*. 105:3903–3908.
22. Malek, A., E. Bakhidze, A. Noske, C. Sers, A. Aigner, et al. 2008. HMGA2 gene is a promising target for ovarian cancer silencing therapy. *Int. J. Cancer*. 123:348–356.
23. Miao, Y., T. Cui, F. Leng, and W. D. Wilson. 2008. Inhibition of high-mobility-group A2 protein binding to DNA by netropsin: a biosensor-surface plasmon resonance assay. *Anal. Biochem*. 374:7–15.
24. Bustin, M. 2001. Revised nomenclature for high mobility group (HMG) chromosomal proteins. *Trends Biochem. Sci*. 26:152–153.
25. Lehn, D. A., T. S. Elton, K. R. Johnson, and R. Reeves. 1988. A conformational study of the sequence specific binding of HMG-I (Y) with the bovine interleukin-2 cDNA. *Biochem. Int*. 16:963–971.
26. Huth, J. R., C. A. Bewley, M. S. Nissen, J. N. Evans, R. Reeves, et al. 1997. The solution structure of an HMG-I(Y)-DNA complex defines a new architectural minor groove binding motif. *Nat. Struct. Biol*. 4:657–665.
27. Fedele, M., R. Visone, I. De Martino, G. Troncone, D. Palmieri, et al. 2006. HMGA2 induces pituitary tumorigenesis by enhancing E2F1 activity. *Cancer Cell*. 9:459–471.
28. Vallone, D., S. Battista, G. M. Pierantoni, M. Fedele, L. Casalino, et al. 1997. Neoplastic transformation of rat thyroid cells requires the junB and fra-1 gene induction which is dependent on the HMGI-C gene product. *EMBO J*. 16:5310–5321.

29. Thomae, A. W., D. Pich, J. Brocher, M. P. Spindler, C. Berens, et al. 2008. Interaction between HMGA1a and the origin recognition complex creates site-specific replication origins. *Proc. Natl. Acad. Sci. USA.* 105:1692–1697.

30. Reeves, R., and J. E. Adair. 2005. Role of high mobility group (HMG) chromatin proteins in DNA repair. *DNA Repair (Amst.).* 4:926–938.

31. Cui, T., and F. Leng. 2007. Specific recognition of AT-rich DNA sequences by the mammalian high mobility group protein AT-hook 2: a SELEX study. *Biochemistry.* 46:13059–13066.

32. Cui, T., S. Wei, K. Brew, and F. Leng. 2005. Energetics of binding the mammalian high mobility group protein HMGA2 to poly(dA-dT)2 and poly(dA)-poly(dT). *J. Mol. Biol.* 352:629–645.

33. Cui, T., S. Joynt, V. Morillo, M. Baez, Z. Hua, et al. 2007. Large scale preparation of the mammalian high mobility group protein A2 for biophysical studies. *Protein Pept. Lett.* 14:87–91.

34. Marky, L. A., and K. J. Breslauer. 1982. Calorimetric determination of base-stacking enthalpies in double- helical DNA molecules. *Biopolymers.* 21:2185–2194.

35. Vesnaver, G., and K. J. Breslauer. 1991. The contribution of DNA single-stranded order to the thermodynamics of duplex formation. *Proc. Natl. Acad. Sci. USA.* 88:3569–3573.

36. Erie, D. A., R. A. Jones, W. K. Olson, N. K. Sinha, and K. J. Breslauer. 1989. Melting behavior of a covalently closed, single-stranded, circular DNA. *Biochemistry.* 28:268–273.

37. Rentzeperis, D., K. Alessi, and L. A. Marky. 1993. Thermodynamics of DNA hairpins: contribution of loop size to hairpin stability and ethidium binding. *Nucleic Acids Res.* 21:2683–2689.

38. Riccelli, P. V., J. Hilario, F. J. Gallo, A. P. Young, and A. S. Benight. 1996. DNA and RNA oligomer sequences from the 3′ noncoding region of the chicken glutamine synthetase gene from intramolecular hairpins. *Biochemistry.* 35:15364–15372.

39. Fodor, E., and A. Ginsburg. 2006. Specific DNA binding by the homeodomain Nkx2.5(C56S): detection of impaired DNA or unfolded protein by isothermal titration calorimetry. *Proteins.* 64:13–18.

40. Freyer, M. W., R. Buscaglia, B. Nguyen, W. D. Wilson, and E. A. Lewis. 2006. Binding of netropsin and 4,6-diamidino-2-phenylindole to an A2T2 DNA hairpin: a comparison of biophysical techniques. *Anal. Biochem.* 355:259–266.

41. Freyer, M. W., R. Buscaglia, A. Hollingsworth, J. Ramos, M. Blynn, et al. 2007. Break in the heat capacity change at 303 K for complex binding of netropsin to AATT containing hairpin DNA constructs. *Biophys. J.* 92:2516–2522.

42. Freyer, M. W., R. Buscaglia, D. Cashman, S. Hyslop, W. D. Wilson, et al. 2007. Binding of netropsin to several DNA constructs: evidence for at least two different 1:1 complexes formed from an -AATT-containing ds-DNA construct and a single minor groove binding ligand. *Biophys. Chem.* 126:186–196.

43. Jen-Jacobson, L., L. E. Engler, and L. A. Jacobson. 2000. Structural and thermodynamic strategies for site-specific DNA binding proteins. *Struct. Fold. Des.* 8:1015–1023.

44. Chalikian, T. V., G. E. Plum, A. P. Sarvazyan, and K. J. Breslauer. 1994. Influence of drug binding on DNA hydration: acoustic and densimetric characterizations of netropsin binding to the poly(dAdT).poly(dAdT) and poly(dA).poly(dT) duplexes and the poly(dT).poly(dA).poly(dT) triplex at 25 degrees C. *Biochemistry.* 33:8629–8640.

45. Herrera, J. E., and J. B. Chaires. 1989. A premelting conformational transition in poly(dA)-Poly(dT) coupled to daunomycin binding. *Biochemistry.* 28:1993–2000.

46. Sharp, K. 2001. Entropy-enthalpy compensation: fact or artifact? *Protein Sci.* 10:661–667.

47. Liepinsh, E., G. Otting, and K. Wuthrich. 1992. NMR observation of individual molecules of hydration water bound to DNA duplexes: direct evidence for a spine of hydration water present in aqueous solution. *Nucleic Acids Res.* 20:6549–6553.